JOINT EUROPEAN TORUS

JET–P(88)57

J. Ehrenberg, P. Coad, L de KocK, S.K. Erents, A. Gondhalekar, D. Goodall, J. Hancock, P. Harbour, T.T.C. Jones, G. McCracken, P. Morgan, C. Nicholson, G. Neill, J. O'Rourke, J. Partridge, M. Pick, J. Simpson, K. Sonnenberg, A. Stevens, M. Stamp, P. Stott, D. Summers, T. Tagle and J. Vince

Hydrogen and Helium Recycling in Tokamaks with Carbon Walls

Hydrogen and Helium Recycling in Tokamaks with Carbon Walls

J. Ehrenberg, P. Coad, L de KocK, S.K. Erents, A. Gondhalekar, D. Goodall, J. Hancock, P. Harbour, T.T.C. Jones, G. McCracken, P. Morgan, C. Nicholson, G. Neill, J. O'Rourke, J. Partridge, M. Pick, J. Simpson, K. Sonnenberg, A. Stevens, M. Stamp, P. Stott, D. Summers, T. Tagle and J. Vince

JET-Joint Undertaking, Culham Science Centre, OX14 3DB, Abingdon, UK

Preprint of an Invited Paper presented at the 8th International Conference
on Plasma Surface Interactions in Controlled Fusion Devices,
2nd May – 6th May 1988, Jüllich, F.R.G.

8th International Conference on Plasma-Surface-Interactions in Controlled Fusion Devices, 2-6 May 1988, Jülich, FRG

HYDROGEN AND HELIUM RECYCLING IN TOKAMAKS WITH CARBON WALLS

J Ehrenberg

with contributions from: P Coad, L de Kock, S K Erents, A Gondhalekar, D Goodall, J Hancock, P Harbour, T T C Jones, G McCracken, P Morgan, C Nicholson, G Neill, J O'Rourke, J Partridge, M Pick, J Simpson, K Sonnenberg, A Stevens, M Stamp, P Stott, D Summers, T Tagle, J Vince

JET Joint Undertaking, Abingdon, Oxfordshire, OX14 3EA, UK

Keywords: Tokamaks, Recycling, Wall pumping

ABSTRACT

This paper presents a review of hydrogen and helium recycling phenomena in tokamaks with limiters and walls largely made out of carbon (graphite, a-C:H layers). The key points of interest are the plasma fuelling efficiency, the wall pumping phenomena as observed in JET, TFTR, TEXTOR and other machines under various fuelling schemes (gas, neutral beams, pellets), the release of hydrogen/helium from material surfaces during and after plasma discharges and the long term retention (total particle inventory) of hydrogen in graphite or carbonised structures in tokamaks. The effect of a combined hydrogen/helium plasma on recycling is also discussed. It is shown that only part of the above phenomena can be understood in terms of processes between hydrogen/helium and carbon as known from simulation experiments (ion beams, gas discharge facilities) and that others (in particular the JET wall pumping phenomenon) have still to be explained. Possible mechanisms are outlined and discussed by means of global models.

I INTRODUCTION

The interaction of the plasma with material surfaces in tokamaks and the release of the fuel gas from them back into the plasma, usually denoted by the term recycling, has important consequences on the plasma energy balance, the plasma particle balance, and also on the relevant material properties (uptake and release of fuel gas). Several articles have been written on these issues, for instance /1,2,3,4,5,6,7/.

Some examples may illustrate this in more detail. In TFTR /8,9/ particularly low plasma densities were achieved for high-temperature neutral-beam heated experiments by conditioning the limiter such that the recycling of particles was reduced (limiter pumping). In D-III D, the energy confinement time of H-modes was improved by about 15% to 20% after the walls/divertor plates had been conditioned such that they pumped hydrogen /10/. The control of particle recycling and, therefore, plasma density is also important because too high a plasma density can give rise to density limit disruptions /11,12/ which, for machines with plasma currents of several MA's as in JET, can be a risk for the integrity of the vacuum vessel.

Because of future deuterium-tritium operations at JET and TFTR, studies are undertaken /13/ to optimise $Q = \frac{P_t}{P_{Heat}}$ (where P_t total fusion power; P_{Heat}: total heating power) by producing peaked density profiles enabling better neutral beam and pellet penetration to the plasma centre. Peaking can be considerably improved if the particles are being pumped away from the plasma edge rather than allowed to recycle into it /13/. Optimizing Q also demands a plasma where the deuteron concentration is equal to the triton concentration. It is known from H to D isotopic exchange experiments in tokamaks /1/ that, to establish a specific plasma isotope ratio needs several previous conditioning discharges are needed. The number of these discharges as well as their isotope composition depend strongly on the limiter and wall materials in question and their ability to take up and release the fuel gas. The release of the fuel gas from material surfaces after the plasma discharge is important for the assessment of the tritium inventory and distribution in the vacuum vessel.

Historically, materials for limiters and walls of a tokamak were selected according to their practicality and to reduce core plasma energy losses by impurity radiation. Consequently plasma-exposed surfaces like limiters which were initially made out of metals were later built out of the lower Z carbon. However, plasma operation contaminated the limiters with wall materials (metals), thus, reducing the benefits of the low Z material. To remedy this situation the walls were partially covered by carbon tiles and in some machines (for instance TEXTOR, JET, ASDEX) a carbon layer was deposited onto the walls by means of a glow discharge with H_2 (D_2) and methane (carbonisation) /14/. In table 1 the relative coverage of some tokamak walls with carbon is indicated.

The change of materials from metals to carbon affected also the recycling of the plasma fuel. The main difference was that less gas was required to set up a constant density in a machine with a carbon limiter /15/. Furthermore, plasma fuelling by uncontrolled gas release from limiters/walls became a common problem in carbon tokamak operation. Although much work has been done to investigate basic hydrogen and helium interactions with carbon in simulation experiments /5,16/ only comparatively little quantitative application has been made of these results in tokamak recycling studies. A major reason is that recycling phenomena in tokamaks are not only the result of (several) material properties but also of the particle transport in the main plasma as well as of the conditions (temperature, density) in the plasma scrape-off layer (SOL). Isolation of the effect of the material requires a good knowledge about the plasma and the SOL which is, however, often very poor. Furthermore recycling processes in the plasma, the SOL, and on material surfaces are not independent of each other. Therefore one has to be very cautious in comparing recycling phenomena from different machines.

A comprehensive presentation of all the recycling phenomena, even when constrained to carbon machines, would be beyond the scope of this work. Instead this work presents in more detail some issues which have recently gained increased interest, as for example the wall pumping and wall fuelling behaviour under various operational conditions. The aim is to identify possible plasma surface interaction mechanisms from the observed phenomena. The discussion in section III is concentrated on theoretical investigations of those experimental phenomena which cannot be explained by known processes between the plasma fuel and carbon.

II RECYCLING PHENOMENA

II.1 Wall and Limiter Conditions and their Effects on the Plasma Density in Ohmically Heated Discharges

II.1.1 Effect of Wall/Limiter Temperatures

In this section discharges are examined in which walls/limiters and plasma have come close to an equilibrium state (quasi steady state) indicated by the fact that reproducible discharges (density, fuelling) can be performed. A thorough study of the effect of different wall/limiter temperatures on the global recycling of hydrogen has been undertaken in TEXTOR /17,18/. The TEXTOR wall had been carbonized about 1000 discharges before the experiments were carried out and the wall (liner) and limiter were baked each night at about 350°C and 400°C, respectively.

Running the machine at 150°C/270°C for wall/limiter-temperature, respectively a flat top density could be produced during the current flat top as indicated in figure 1a). The gradual density decrease from shot to shot was explained /19/ as a result of the depletion of hydrogen in the carbon limiter by thermal desorption at the end of the foregoing discharge and subsequently increased trapping during the next discharge.

When the wall and limiter temperatures were raised to 350°C and 370°-400°C, respectively, the plasma density decayed already during the current flat top phase (figure 2a), indicating an increased retention of particles in the walls/limiters. A variation of just the limiter temperature (150°-330°C) did not markedly alter the results, suggesting the carbonised wall being the dominant density controlling material surface in TEXTOR. TFTR ohmic discharges with walls and (inner bumper) limiters at about room temperature showed also a near flat-top density during the current flat-top phase /8/. If the external gas supply is switched off the density decays with an initial time constant τ_p^* larger than 10s. τ_p^* is defined as:

$$\dot{N}_p = -\frac{N_p}{\tau_p} + R(t)\,\frac{N_p}{\tau_p} \qquad (1)$$

$$\tau_p^* = \frac{\tau_p}{1 - R(t)} = -\frac{N_p}{\dot{N}_p} \qquad (2)$$

with N_p: total plasma particle (electron) inventory,

τ_p: global particle confinement time, depends on plasma transport and particle source distribution in the plasma.

R(t): global recycling coefficient.

Ohmic discharges in JET with the eight discrete limiter configuration of 1986, however with a limiter and wall temperature of 300°C also showed nearly flat top density during the current flat top phase. τ_p^* was larger than about 400 s, figure 3a). Using a six times larger and actively cooled belt limiter instead, τ_p^* changed to about 11 s, figure 3b. However the limiter temperature was also changed to about 150°C. Discharges with the belt limiter at 300°C were also performed at the start of the experimental campaigns of 1987 and 1988 and τ_p^* was measured to be much larger ($\gtrsim$ 100 s). However, previous to these campaigns extensive hydrogen glow discharge cleaning was performed which makes interpretation ambiguous (see next section). In contrast to TEXTOR the dominant interactions between plasma and material surfaces in JET and TFTR take place at the limiters. Comparison between JET and TEXTOR results indicate an increased pumping capacity at higher temperatures in TEXTOR, and the opposite in JET. It is an open question as to whether this is due to a genuine difference between the solid carbon (JET) limiter and the carbonized metal wall (TEXTOR). Comparison between JET and TFTR indicates similar results for τ_p^*, although temperatures were quite different suggesting either differences of the hydrogen storage capacity of the different types of graphites, or indicating no temperature dependency.

It is important to note that for a more detailed analysis the effect of the different particle fluxes to the different surfaces in the tokamaks (limiter, walls) have to be established. The global recycling is easily controlled by the pumping of only 10% of the particle efflux from the plasma, which would give a global particle recycling coefficient of 0.9. Even assuming a large particle confinement time of 0.5 s the plasma density would then be reduced by 20% in 1 s which is still large compared to what is observed in figures 1-3. However the important result derived from the above phenomena is, that even when reproducible discharge are possible, a continuous particle loss occurs whose magnitude seems to depend on wall/limiter temperature. This is, reminiscent of the recycling behaviour of hydrogen in metal machines (particle losses into the bulk material); however other processes like carbon-hydrogen codeposition would also explain such a result (see section III).

A rough but useful quantity for measuring the particle up-take of the walls/limiters during a plasma discharge is the fuelling ratio F:

$$F = \frac{N_e^p}{N_e^{in}}$$

where N_e^p = total plasma electron content at time t in the discharge, and $N_e^{in} = \int_0^t \phi_{ex}\, dt$: total external electron input until time t, ϕ_{ex} = external electron influx. A correction for Z_{eff} of the discharge gives the hydrogenic plasma content. The ratio F is given in figure 4 as a function of N_e^{in} for JET belt limiter discharges. It decreases with increasing N_e^{in} even if corrected for Z_{eff}. A very similar result has been obtained for 1986 JET limiter discharges (discrete limiter) as well as for 1986 inner wall discharges /20/. Furthermore, transforming TFTR fuelling efficiency results for hydrogen and deuterium discharges /8/ into a similar functional dependence of F on N_e^{in} gives qualitatively very similar results. Also, JT-60 limiter discharges (TiC-coated graphite) indicate a decrease of the fuelling ratio within the discharge itself as long as the external gas dosing is switched on /21/. This demonstrates that under quasi steady state conditions between plasma and limiter/walls a relatively larger fraction of the input gas ends up in the walls at larger inputs. It has to be borne in mind that this is not a trapping effect as known from implantation experiments /22/ because this effect would cause the fuelling ratio to become 1 after saturation has been reached. Also, the limiter and walls in the above experiments are most likely already saturated /23/.

II.1.2 Effect of a Previous Hydrogen Glow Discharge Cleaning (H-GDC)

Figures 1 and 2 indicate the effect of a previous H-GDC on the plasma density of TEXTOR discharges for two different wall temperatures. At T_W= 150°C the density is increased compared to the same discharge without a previous GDC, indicating H-release from walls due to the previous wall loading. At T_W = 350°C no such increased plasma density is measured (figure 2b) /17/ indicating no wall loading by a GDC at that temperature. Experiments in JET with walls and limiters at about 300°C show also an initially increased plasma density which decreases during the course of a discharge series. Figure 5 indicates the fuelling ratio for such discharges as a function of the total number of input electrons. It shows that in this case after about four to five discharges a quasi steady state has been reached similar to the one indicated in figure 4, although temperatures were different. Both JET (at 300°C) and TEXTOR (at 150°C) results also indicate that the hydrogen loading of material surfaces during H-GDC must be different from the loading which occurs during tokamak discharges. After GDC the wall seems to be supersaturated relative to the equilibrium state produced by a tokamak discharges. Then, during discharges plasma induced desorption depletes the walls of hydrogen. It is not clear whether wall/limiter temperatures in JET around 350°C would give a similar results as in TEXTOR where no wall loading is observed or whether this is again due to a genuine difference between carbonised metal walls and solid carbon.

II.1.3 Changeover from Hydrogen to Helium

It is well known that changing the gasfil of a tokamak from hydrogen to deuterium does not result in corresponding and immediate change of the plasma fuel (see for example /24,25,26/). Similar results are obtained during the change over to helium with the additional effect of the plasma density being increased by hydrogen desorption from walls/limiter during the initial helium fuelled discharges. Figure 6 gives an example from JET with data taken from discharges with $T_L \approx T_W \approx 200$°C as well as $T_C \approx T_W \approx 300$°C. Due to differences in the discharges differences between the fuelling ratios at two wall temperatures cannot be judged to be caused by the change of temperatures. The common feature is that helium releases hydrogen from walls/limiters and that the depletion of it causes the fuelling ratio to decrease with progressive discharges (helium wall conditioning /9/). Helium itself is apparently not being pumped by these material surfaces since the fuelling ratio stays approximately at one (compare discharge No 34 with No 53). This is very similar to TFTR He-discharge results where the fuelling ratio was 1 although the walls were at about room temperature and only the (movable) limiter was at about 300°C /8/. The release of hydrogen appears to depend on the density of the discharge such that lower densities give rise to a relatively larger release than higher densities (compare discharge No 16,45,53 in figure 6).

It is known from implantation experiments of helium into graphite /27/ that above about 200°C trapping of He is negligeable compared to hydrogen trapping. When saturation is reached one should therefore expect no further retention and therefore a fuelling ratio of 1. Comparing this result with the corresponding hydrogen results of section II.1.1 it can be again concluded that besides trapping of hydrogen an additional hydrogen retention mechanism is taking place which is absent or much weaker for helium, and which puts the hydrogen fuelling ratio to below one (see also section III).

II.1.4 Changeover from Helium to Hydrogen

As described in the previous section, Helium discharges can desorb hydrogen from walls and therefore subsequent discharges in hydrogen experience increased pumping by walls/limiters. Figure 7 gives an example from TFTR /8,9/ without and with previous helium conditioning. The decrease of τ_p^* to about 2 s is due to a decrease of the global particle recycling coefficient (see equation 2). It is also indicated in figure 7 that the external gas feed has increased to set up the required plasma density after the conditioning. Both effects decrease with progressive hydrogen discharges indicating that walls and limiter are getting saturated. The TFTR inner limiter was estimated to retain about 100 Torr.ℓ of hydrogen /9/. Very similar qualitative results have been obtained after JET helium charges where strong hydrogen pumping is a common feature of the initial hydrogen discharges and after outgassing of the TEXTOR walls /18/.

II.2 Variation of the Plasma Position and its Effects on the Plasma Density in Ohmically Heated Discharges (Inner Wall Pumping)

II.2.1 Temperature Dependencies

If the plasma in JET is moved from the outboard limiter to the inner wall the plasma density decreases /3,28/. However, the same thing happens when the plasma is elongated such that it is bounded by the top and bottom carbon tiles of the JET vessel. Examples are given in figure 8 for discharges which were identical (density, current, fuelling) up to the start of the plasma position change (at 6 s). At 10 s in figure 8 the plasma was moved back to the limiter causing a rise of the plasma electron content. Measurements of Z_{eff} via Bremssrahlung indicated that the electron content variation was due to hydrogen content changes.

Such experiments with the belt limiter configuration were performed at T_l = 120°C, T_W = 200°C and with the old discrete limiter configuration at $T_l \approx T_W \approx$ 300°C. However due to different discharge waveforms only a qualitative comparison is possible, indicating no differences between the results of the two series. Inner wall or top/bottom pumping has been observed in JET under all combinations of limiter and wall temperature: T_l = 120°C T_W = 200°C; T_l = 300°C, T_W = 300°C; T_l = 200°C, T_W = 200°C; T_l = 150°C, T_W= 300°C. Figure 8 indicates that pumping is even stronger at the top/bottom than at the inner wall. How a change in flux density causes the pumping is not clear: Inner wall and belt limiter in JET have about similar areas but magnetic compression of flux surfaces at the outside versus inside contributes to smaller scrape off decay lengths at the outside (see III.4). However, the perpendicular diffusion coefficient in the plasma boundary of inner wall discharges has not been measured so that the real SOL width is not known.

This pumping does also not deteriorate in progressive discharges.

Experiments in TEXTOR /17,29/ show a very similar pump-out of the plasma density when the plasma is moved towards the inside of the vessel, figure 9. At lower temperature (T_W = 150°C) the pump-out seems to be much less pronounced, figure 10a). Similar to JET discharges, no saturation effects are observed. However, it is not clear whether the plasma density would recover if the TEXTOR plasma was shifted back to the outboard limiter.

It has been observed in other machines like TFTR /8/ and PDX /30/, that inner wall discharges require more gas (about 30% and 60%, respectively) to set up the same density as in the outer limiter configuration. This might be an indirect indication for inner wall pumping. Moreover, recent results of TEXT /31/ as well as earlier ones of ASDEX /15/ with stainless steel limiters have shown that there is a recycling asymmetry between the outer and inner limiter. The TEXT results are interpreted as a reduction of the global particle confinement time when the plasma leans at the inboard wall. It will be discussed in more detail in section III that this can cause a density drop without a change of wall properties.

II.2.2 Effect of Previous H-GDC

Similarly to the results in section II.1.2 a hydrogen loading of the walls by a hydrogen GDC can lead to an increased density even in inner wall discharges and thus to a suppression of the pumping effect as is indicated in figure 10 b,c) for a wall temperature of 150°C in TEXTOR.

II.2.3 Effect on He Discharges

If the walls of JET are sufficiently depleted of hydrogen by previous helium discharges such that the hydrogen content in the plasma is about 15% or less of the electron content, inner wall pumping in helium fuelled discharges is much weaker than in hydrogen fuelled ones, figure 11. In fact its magnitude could be entirely attributed to the pump out of the residual hydrogen in the plasma. This result is consistent with the observations indicated by figure 6, that helium is not or only weakly pumped in graphite at temperature of about 200°-300°C.

II.2.4 Effect on Hydrogen Discharges after He Discharges

A depletion of hydrogen in the inner walls can cause an increased pumping capacity of it in subsequent inner wall hydrogen discharges. This pumping enhancement, however, deteriorates with progressive discharges indicating a saturation effect. The 'normal' wall pumping is then restored. An example from JET is given in figure 12a) where the gas fuelling (figure 12b) was switched on when the plasma was moved to the inboard wall except in # 12603 which was the fifth discharge in deuterium after eleven discharge in helium. In TFTR specifically low density H-discharges were performed at the inner bumper limiter after He-conditioning /8,9/.

II.3 Recycling Phenomena in Auxiliary Heated and Core Fuelled Discharges

II.3.1 Effect of Neutral Beam Heating

The density evolution during neutral beam heating can be divided into two phases /8,20/. First is an initial phase from the onset of the beams until a time which corresponds roughly to a confinement time for core fuelled particles (0.5- 1 s in JET) and second is a later phase thereafter. Figure 13 indicates these two phases for neutral beam fuelling under various conditions in JET. In phase I the density rises according to the beam fuelling (ϕ_{beam}) or even faster whereas in phase II the density rise decreases or even stops (density clamping). The reason for the increased (over the beam fuelling) density rise is desorption of hydrogen from walls and limiters which is absent if previous He discharges have depleted the walls of hydrogen (compare a) and b) in figure 13). Direct evidence of hydrogen desorption during neutral beam fuelling has been obtained in the JFT-2M Tokamak /32/ where during a deuterium plasma discharge in a vessel with hydrogen conditioned walls the hydrogen and deuterium partial pressures were measured simultaneously. During the beam heating phase only the hydrogen pressure increased, figure 14c).

In phase II particle loses from the plasma to the walls and limiters dominate.

The density can continue to rise which can be explained (figure 13a) by assuming an increase of the particle content in both, the plasma and the wall/limiters and a mutual exchange of particles between these two reservoirs /20/. With He-conditioned walls the loss of particles from the plasma equals the beam fuelling plus any possible wall fuelling. The removal of particles in this case is permanent at least for the duration of the additional heating phase. It could be suggested that this is related to the increased retention efficiency of the walls (trapping) after the conditioning. However density clamping is also observed in JET X-point discharges <u>without</u> He conditioning. Also, TFTR neutral beam heated discharges exhibit a similar density behaviour explained as a consequence of the reduction of the global recycling coefficient, decreasing with increasing beam power /8/.

As to be pointed out in section III and mentioned already above a possible degradation of the plasma particle confinement can also cause a density decrease without changing the wall properties. However the wall has to be in a state where it can retain particles.

II.3.2 Effect of RF Heating

Although RF heating is supposed to deposit only energy into the plasma it is well known that with the use of graphite limiters desorption of hydrogen and consequently an increase of the density also occurs (for instance /33/). Examples are shown in figure 14.

A detailed analysis of this phenomena by Bures et al /34/ concluded two release processes of hydrogen from walls/limiters to be responsible for the density increase: Firstly a fast (ms) release at the onset of RF heating and secondly a slower one thereafter possibly associated with the increased power flow into the plasma scrape-off layer during heating. In both cases is the particle release roughly proportional to the RF-power. Similar to the case of neutral beam heating, the increase of the density persists only as long as the auxiliary heating is switched on and the density rapidly (1 s) decays afterwards to a value which is about as low or even lower as before heating.

II.3.3 Effect of Pellet Injection

Pellet fuelled discharges are characterised by a rapid (ms) increase of the electron content corresponding to the ablation process and a subsequent pump out. The pump out can be rapid < 1 s or slow (> 1 s) without having changed the wall conditions and seems strongly related to changes of the particle transport, as for example the occurrence of MHD locked modes /35/ which are usually followed by a rapid pump out. However again the wall limiters must have the capacity of retaining the particles in order to keep the density low.

II.4 Particle Release after Plasma Discharges

Hydrogen outgassing in tokamaks with stainless steel walls, as for instance in ASDEX, is known to recover almost all ($\gtrsim$ 90%) of the particles (within about 15 min) which had been admitted into the machine /36/. Carbonising the walls has decreased this fraction to much lower values (< 50%) /37/. Particle balance measurements in TFTR indicate that without helium conditioned walls only about 25% of the input gas is desorbed from the walls after a discharge /38/. Similar measurements in JT-60 (TiC walls) show that for ohmic discharges 40%-80% of the admitted gas leaves the walls /33/. Ohmic discharges in JET indicate that typically only 20% ± 10% are released within 10^3 s after the discharge /40/ if the discharge ended with a soft landing of the plasma current. Disruptive discharges clearly show a release fraction which is much larger (between 50% and 200%) (figure 15) suggesting that larger power depositions on to walls cause thermal desorption of hydrogen. Helium discharges end almost always in disruptions, indicating little He pumping by walls. Current investigation in JET also suggest that even in additionally heated and pellet fuelled discharges the fraction of released particles to those admitted by the gas puff does not markedly change.

The slow outgassing from JET walls is indicated by the temporal variation of the total gas pressure (80% H_2 (or D_2)) figure 16. The two examples were taken from discharges with different wall temperatures (# 14076: T_l = 150°C, T_W = 300°C; # 12009: T_l = 120°C, T_W = 200°C).

However these differences between the data are not specifically larger than the scattering of data from different discharges with the same wall temperature. Therefore, a temperaure dependance cannot be derived. Taking into account the pumping time constant of 20 s for hydrogen a calculated wall release process with release time constants of the order of 10 s, 100 s, and 1000 s can well approximate the measured data.

It is conclusive to compare these release time constants with release times of particles from walls during discharges (figure 8) indicating that the latter are typically one second or less, for instance when the plasma is moved from the inner wall back to the limiter. [The plasma is a pump for wall released hydrogen with a time constant much shorter than 20 s]. This suggests that release processes with and without plasma are quite different (at least in JET) making it rather difficult to derive particle release mechanisms which take place during the discharge from the observation of the outgassing behaviour afterwards.

II.5 Summary of Recycling Phenomena

The data which were presented in the last four sections can be summarized as follows:

1) The fuelling ratio as defined in section II.1.1 for hydrogen/deuterium plasmas in carbon rich tokamaks with hydrogen discharge conditioned walls is smaller than one and decreases with increasing input (density). This indicates that a large proportion of the input gas is staying in the walls/limiter but exchanges particles with the plasma. This has been observed at $T_l \approx T_W \approx$ 30°C (TFTR) and $T_l \approx T_W \approx$ 300°C (JET).
2) A H(D)-GDC prior to a tokamak discharge increases the fuelling ratio above one for the initial discharges (JET, $T_l \approx T_W \approx$ 150-300°C), TEXTOR T_W = 150°C indicating plasma induced hydrogen desorption from walls/limiters. No such effect has been observed at T_W = 350°C in TEXTOR.
3) Change over from hydrogen to helium discharges even without previous H-GDC also increases the fuelling ratio above one indicating helium-induced hydrogen desorption. In contrast to hydrogen discharges, helium-conditioned helium discharges have a

fuelling ratio of about one indicating relatively little helium pumping (JET, TFTR).

4) Change over from helium to hydrogen discharges requires more gas to obtain the same density than under the conditions of 1) indicating increased wall/limiter pumping due to H-trapping. However this additional effect deteriorates with progressive discharges indicating hydrogen saturation in walls/limiters (JET, TFTR), at least on the time scale of days.

5) Hydrogen discharge conditioned walls at 150°C in TEXTOR exhibit clearly less pumping than at 350°C. This result possibly contrasts with observations in JET where at a limiter/wall temperature of 300°C/300°C the pumping seems to be less than at 150°C/300°C.

6) Hydrogen pumping caused by plasma position changes (outer limiter to inner wall) does not deteriorate and can be increased by pre He-conditioning. Results from TEXTOR indicate that at T_W = 350°C the pumping is larger than at 150°C. An important feature is that the wall refuels the plasma if it is moved back to the limiter (JET).

7) Auxiliary heating of discharges with hydrogen conditioned walls leads to a desorption of wall/limiter hydrogen (JFT-2M), which in case of RF heating is roughly proportional to the applied power (JET).

8) Wall/limiter outgassing after discharges results in a hydrogen recovery fraction ≤ 50% of the input gas. (JET, TFTR, JT60). The recovery fraction is higher (→ 200%) after disruptive discharge (JET).

9) The outgassing time constants after discharges with soft current termination landing are about an order of magnitude or more larger than outgassing time constants during plasma discharges (JET).

III DISCUSSIONS

III.1 General Concept

It has been said already that the various recycling phenomena presented in the foregoing paragraph are not always only a consequence of the state of the limiter and walls, but that the plasma transport and the conditions (temperature, density, transport) in the plasma boundary and scrape-off layer can have also an important effect on recycling. To describe recycling phenomena and to make predictions a model of all three components, plasma, plasma boundary, and wall would be required and has already been developed by several authors, for example /6,7,41,42/.

It is beyond the scope of this paper to discuss the recycling phenomena in the light of these detailed models also because much of the relevant data, in particular from the plasma boundary, are not known. Instead a more global approach is pursued which may suffer from simplifications but can nevertheless give some insight into the recycling processes.

Figure 17 indicates a simple view of the three particle reservoirs in a tokamak between which particles recycle: the plasma, the plasma boundary and SOL, and the wall/limiter (denoted by subscript P,B,W respectively). It is assumed that particles which leave the plasma end up at walls and limiters and that particles leaving these surfaces and entering the SOL or boundary have a probability f to refuel the plasma whereas a fraction (1-f) may go back to material surfaces.

This shall take into account for example ionisation of neutral particles within the SOL or charge exchange losses to the wall both of which would reduce the fuelling efficiency.

It is further assumed that the total number of particles, which is the sum of the individual particle inventories is constant. Thus:

$$N = N_W + N_B + N_p = \text{const} \tag{1}$$

The fluxes out of the individual reservoirs are governed by the respective particle confinement times which in turn are dependent on the individual transport processes in these reservoirs. According to figure 17 the three reservoirs can be connected to each other by three simple differential equations:

$$\dot{N}_p = -\frac{N_p}{\tau_p} + f\,\frac{N_B}{\tau_B} \tag{2}$$

$$\dot{N}_B = -\frac{N_B}{\tau_B} + \frac{N_W}{\tau_W} + r\frac{N_p}{\tau_p} \quad (3)$$

$$\dot{N}_W = -\frac{N_W}{\tau_W} + (1-r)\frac{N_p}{\tau_p} + (1-f)\frac{N_B}{\tau_B} \quad (4)$$

r: reflection coefficient

In steady state N_p reads:

$$N_p = \frac{f \cdot \tau_p}{\tau_W\ (1-r \cdot f)\ + \tau_B + f\tau_p} N \quad (6)$$

II.2 Estimate of the Confinement Times for JET Discharges

Global plasma particle confinement times are often determined by density and Hα-measurements /6,7/ and τ_p is calculated from:

$$\dot{N}_p = -\frac{N_p}{\tau_p} + \sum \phi_{in} \quad (7)$$

where ϕ_{in} are all the fluxes into the plasma measured by Hα spectroscopy. One can estimate an average reflection coefficient according to T_e measurements by Langmuir probes (for latest JET results see /43/). For a machine like JET $\tau_p \approx 0.2$ s for medium density discharges and $r \approx 0.5$ (D onto carbon).

Assessing values for f is much more difficult as it depends on the atomic processes and plasma transport in the plasma boundary as well as on the geometrical conditions of the plasma limiting surface. If ionisation within the SOL is the major process to reduce the fuelling efficiency one can, as an example, easily calculate values for f. It is assumed that the wall is at a radial position x=0, that the limiter is at $x=\ell$ and that the starting point for a recycling neutral hydrogen molecule which moves radially towards the plasma is at x=a. Moreover, it is also assumed that there is an exponentially decaying electron density in the SOL and $0 < a < \ell$ then:

$$f = \exp\left(\frac{-\lambda_n}{d}\left(1 - \exp^{-(\ell-a)/\lambda_n}\right)\right) \tag{8}$$

with

$$d^{-1} = \frac{\langle \sigma \cdot v_e \rangle \cdot n(a)}{v_n}$$

where v_n: velocity of a thermal neutral molecular hydrogen ($\approx 10^3 \frac{m}{s}$)
$\langle \sigma \cdot v_e \rangle$: ionisation rate coefficient ($4 \cdot 10^{-14} \frac{m^3}{s}$), ($T_e \geq 20$ eV).
n(a) electron density at plasma boundary ($\approx 10^{18}$ m^{-3})
λ_n: density SOL width (0.015 m, at the JET limiter)
λ_T: temperature SOL width (see below)

The particle flux which hits the plasma limiting surface has a decay length of $\lambda = \frac{2\lambda_n \lambda_T}{2\lambda_T + \lambda_n}$. For $\lambda_T \approx \lambda_n$, $\lambda = \frac{2}{3}\lambda_n$. The radial position $a = \ell - \lambda$ on this surface can be used as an average starting point for recycling neutral particles. Thus $f \approx \exp-\left(\frac{\lambda_n}{2d}\right)$. With $\lambda_n = 0.015$ m and d= 0.025 m then f = 0.7 at the JET limiter. Other processes (charge exchange, Franck-Condon-atom formation) would of course alter this value. With electron temperatures above 20-30 eV in the plasma boundary /4,3/ an estimate of the total fuelling efficiency could be about 0.5 /49/. Thus $(f \cdot \tau_p) \approx 0.1$ s.

The SOL particle confinement time for neutrals can be estimated to be either:

$$\tau_B \lessapprox \frac{\ell - a}{v_n} \quad \text{if } (\ell - a) < \lambda_{ion};\ \lambda_{ion} = \text{mean free path for ionisation}$$

or

$$\tau_B \approx \frac{\lambda_{ion}}{v_n} \quad \text{if } (\ell-a) > \lambda_{ion}$$

For <u>ions</u> $\tau_B \lesssim \frac{L_{||}}{v_{ion}}$

$L_{||}$ typical connection length to limiter
v_{ion} typical ion velocity in SOL

For JET: $\lambda_{ion} \approx 0(10^{-2}\text{m})$, $L_{||} \approx 0(10\text{m})$, $v_n \approx 0(10^3 \frac{\text{m}}{\text{s}})$
$v_{ion} \approx 0(10^5 \frac{\text{m}}{\text{s}})$, $(\ell-a) \approx 0(10^{-1}\text{m})$ thus:
$0(10^{-5}\text{s}) \leq \tau_B \leq 0(10^{-4}\text{s})$

Therefore $f\tau_p \gg \tau_B$, ie. the SOL is a negligeable particle reservoir when compared with the plasma itself.

It is much more difficult to assess τ_w. However using equation (6) and deriving from it the ratio $\frac{N_p}{N}$ gives an estimate about τ_w if N is identified as the total particle input in a plasma, N_e^{in}. This is only valid for stead state wall conditions (see II.1.1) where it can be assumed that the particle desorption from walls or the permanent trapping by them is negligeable compared to N_e^{in}. With $\frac{N_p}{N} \approx 0.2$ for hydrogen discharges in JET (from section II.1.1) and equation (6) one gets:

$$\tau_w \approx 0.5 \text{ s}$$

or, within the uncertainties, it can be assumed that for hydrogen

$$0(\tau_w) \approx 0(f \cdot \tau_p)$$

A similar results has been obtained by Jones et al /20/ from neutral beam experiments in JET.

For He with $\frac{N_p}{N} \approx 1$ one gets, $\tau_w << f \cdot \tau_p$, thus the helium residence time after saturation in the material surface is much shorter than the hydrogen residence time, a result which is consistent with data derived from ion implantation experiments /59/.

III.3 Possible Processes Related to τ_w

According to equation (6) the ratio $\frac{N_p}{N}$ is a function of τ_w and $f \cdot \tau_p$. Once can discriminate two simple cases: one where τ_w = const and therefore independent of the particle flux, $j = \frac{N_p}{A\,\tau_p}$, where A is the surface area hit by the plasma. An example could be diffusion limited release process from limiters walls. Another case is $\tau_w \propto 1/j$ as for instance in a recombination limited release process /46/. Similarly one can assume τ_p = const or alternatively $\tau_p \propto \frac{1}{N_p}$ according to Engelhardt et al /47/ and as also measured in many tokamaks /48/. Therefore there are four different combinations of τ_p and τ_w with four different dependencies of the fuelling ratio $\frac{N_p}{N}$ on N_p and thus on N assuming that $N = N_e^{in}$. The calculated qualitative dependency of $\frac{N_p}{N}$ on N is given in figure 18 for these four cases. Comparison with figure 14 (steady-state wall conditions) indicates that only the case with $\tau_p \propto 1/N_p$ and τ_w = const. produce the experimentally observed functional dependency, hence τ_w the particle residence time in JET material surfaces does not seem to be flux dependent. If the walls/limiter are not in a steady state condition one might still use the above concept but with an altered definition of N:

i) After H-GDC, $N = N_e^{in} + \Delta N_w^R$ where ΔN_w^R is the amount of hydrogen in walls which is released by plasma-induced processes.
ii) After He conditioning or baking of walls $N = N_e^{in} - \Delta N_w^T$ where ΔN_w^T is that part of the particles which is trapped in walls/limiters.

If, under these circumstances, an equilibrium between plasma and walls is reached during a discharge ΔN_w^B and ΔN_w^T can be calculated using equation (6).

$$\Delta N_w^R = g\, N_p - N_e^{in}$$

$$\Delta N_w^T = N_e^{in} - g\, N_p$$

$$\text{with } g = \frac{f \cdot \tau_p + \tau_w(1-r.f)}{f \cdot \tau_p} \qquad \approx 0(2-5) \text{ for hydrogen}$$

Because g > 1 for hydrogen discharges a determination of gained and lost particles by simply subtracting plasma and input inventories from each other under-or overestimates respectively the additionally released or trapped number of particles.

III.4 Application to Inner Wall Pumping

According to equation (6) a decrease in τ_p, (which, however, is not known when changing the plasma position from the outer to the inner limiter for instance) would cause a density decrease similar to one caused by an increase of the particle wall confinement time τ_w. In fact, the insensitivity of JET inner wall pumping to temperature differences between the outer limiter and the inner wall might suggest that the properties of the wall/limter are not the only reason for a density pump-out. (It must be noted, however, that the real surface temperatures during discharges are often not accurately known. Assuming a total wetted area of 20 m² at the inner wall of JET for instance, and 15 m² at the limiter a 2 MA ohmic discharge would raise the surface temperatures by less than 50°C within 10 s).

A decrease of the fuelling efficiency f at the inner wall can also lead to a reduction of the plasma density. The magnetic topology of JET limiter discharges causes a radial expansion of a magnetic edge flux tube by a factor of about 1.6 when going form the outside to the inside and by a factor of about 3 when going from the outside to the top/bottom of the plasma. This leads to a corresponding increase of λ_n

/50/. Using equation (9) this can change the fuelling efficiency due to ionisation of molecular hydrogen within the SOL as follows:

$$\frac{f_{in}}{f_{out}} = \exp\left(-\frac{\lambda_n^{in} + \lambda_n^{out}}{2d}\right) \approx 0.9$$

$$\frac{f_{t/b}}{f_{out}} = \exp\left(-\frac{\lambda_n^{t/b} + \lambda_n^{out}}{2d}\right) \approx 0.6$$

Assuming $\tau_p = 0.2$ s, $r = 0.5$, $\tau_w = 0.5$ s, $f_{out} = 0.7$ and with equation (6) one gets for the reduction of the density:

$$\frac{N_p^{in}}{N_p^{out}} \approx 0.9$$

$$\frac{N_p^{+/b}}{N_p^{out}} = 0.7$$

Hence, this <u>effect</u> alone does not seem to explain all the density decrease at the inner wall but it can explain why pumping in JET is stronger at the top/bottom than at the inside (figure 8) without assuming respectively different wall properties. It can also explain the observed phenomena of a density loss when changing from a limiter plasma to an X-point plasma in JET.

It is important to note that a finite and non zero residence time of particles in the walls is essential because the walls have to retain the particles. The influence of the wall properties is seen in the results of TEXTOR inner wall discharges with H-GDC conditional walls (figures 10b,c) were no pumping but even an increased fuelling is observed. On the other hand assuming in equation (6) that $\tau_w \ll f\tau_p$ then N_p is independent of f, τ_p and wall properties. In such cases no pumping would be expected. This is exactly the result observed in the He discharges where the residual pumping, as indicated in figure 11, was attributed to the pumping of the residual hydrogen. Therefore the observed density reduction in helium discharges could be explained by a decrease of the fuelling efficiency, the effect of which is much stronger for the hydrogen component because its retention time in the walls is much longer.

III.5 Other Recycling Phenomena

i) Hydrogen Wall Loading by H-GDC and Release of H in Plasma Discharges

One can assume that H plasma discharges implant H into carbon until its saturated. For an impact energy of about 150 eV (4.5 kT) at the limiter, saturation is reached at about 3.10^{20} atoms/m². In JET the total limiter area is about 15 m² resulting in 4.5 10^{21} atoms at saturation. The wall area is about 200 m² (projected onto plasma surface) and therefore could retain about 6.10^{22} atoms. Indeed, surface analyses of wall and limiter samples indicate such amounts of retained H or D in JET /23,50,51/ as well as in other machines with carbon walls /8/. A JET plasma inventory is about $2\text{-}3 \cdot 10^{21}$ H-ions. After hundreds of discharges it is therefore very likely that all the surfaces are saturated. Application of H-GDC at not too high a wall temperature (≤ 300°C), however, can increase further the wall inventory (except in TEXTOR at 350°C). There are two possible explanations for this effect. Firstly H-GDC in carbon machines can produce an appreciable fraction (≤ 10%) of hydro-carbons which leads to a carbonisation process building up hydrogen-saturated carbon layers. Heating of these layer by plasma impact can cause hydrogen desorption. Secondly and similarly, implantation of H by the GDC process (≈ 300 eV) and heating of the surface during plasma operation could also result in H desorption. Even though average temperature rises in ohmic limiter discharges in JET are estimated to be assumed to be only about 50°C or less for 2 MA plasmas, it is still enough to decrease the saturation concentration in carbon by about 10% /22/, releasing about 1 x 10^{21} atoms. Furthermore the majority of hydrogen atoms do not desorb from walls when the plasma discharge has ended but stay within the machine (see II.4) and are available for release in later discharges.

ii) Particle Loss by H-C Codeposition Under Quasi-Steady State Conditions

In III.1 it was assumed that the plasma density stays constant without external gas fuelling. This is only approximately fulfilled as shown in II.1. There is a small but non zero continuous particle loss. In metal machines this is a common phenomena and is interpreted as losses to the bulk material by diffusion /4/. Whether such a process is also possible in carbon machines is an open question. Recently /52,53/ simulation experiments have indicated that the retained amount of hydrogen is proportional to the fluence /58/ and that the retention of H in carbonacous films depends strongly on the time interval in between two plasma exposures suggesting refilling of hydrogen depleted surface layers /51/. Transport of hydrogen through porous graphite has been recently measured /60/.

Furthermore the refuelling of the JET plasma after moving it back from the inner wall onto the limiter also supports this hypothesis. On the other hand a quite different mechanism has been suggested after the discovery of thick (tens of µm) hydrogen and saturated carbon films on wall structures /23,50/ of carbon tokamaks. It was assumed that codeposition of H and C onto surfaces which are dominated by deposition rather than erosion /54/ removed hydrogen from the plasma and produced these thick layers. Furthermore, results of a simulation experiment by Hsu et al /55/ were similarly interpreted. A brief calculation demonstrates that this process can indeed be an effective pumping mechanism.

It is assumed that the plasma-surface interaction zones are divided into an erosion zone (e) and a deposition zone (d) /54/. The particle balance equation for hydrogen (N_p) and for carbon (N_c) plasma particles reads then (without external sources):

$$\dot{N}_p = - (C_e + C_d) \frac{N_p}{\tau_p} + R_e C_e \frac{N_p}{\tau_p} + R_d C_d \frac{N_p}{\tau_p} \qquad (10)$$

$$\dot{N}_c = - (C_e + C_d) \frac{N_c}{\tau_c} + Y_c C_e \frac{N_c}{\tau_c} + Y_H C_e \frac{N_p}{\tau_p} \qquad (11)$$

where C_e, C_d are partition factors for particle fluxes onto erosion and deposition dominated zones, respectively. Here they are assumed to be equal for carbon and hydrogen.

τ_p, τ_c respective particle confinement times for hydrogen and carbon.
R_e, R_d hydrogen recycling coefficients in erosion, deposition zone.
Y_c, Y_H selfsputtering and hydrogen sputtering coefficients for carbon.

Assume $R_e = 1$ (no pumping in erosion zone). The carbon flux onto the deposition zone is

$$\phi_c^d = C_d \frac{N_c}{\tau_c} \qquad (12)$$

The hydrogen flux there is:

$$\phi_H^d = C_d \frac{N_p}{\tau_p} \qquad (13)$$

Trapping of hydrogen due to codeposition is assumed such that saturation is reached (relative concentration of hydrogen in carbon ≈ 0.4) (Becaused $\phi_H^d >> \phi_c^d$ this is instantaneously fulfilled).

$$\frac{\phi_H^T}{\phi_c^d} = 0.4 \rightarrow \phi_H^T = 0.4\ \phi_c^d$$

Reemission of hydrogen from the deposition zone is then:

$$\phi_H^R = \phi_H^d - \phi_H^T = C_d \left(\frac{N_p}{\tau_p} - 0.4 \frac{N_c}{\tau_c}\right)$$

with R_d from equation 10:

$$R_d = \frac{\phi_H^R}{C_d \dfrac{N_p}{\tau_p}} = 1 - 0.4 \frac{N_c}{N_p} \frac{\tau_p}{\tau_c}$$

If $\dot{N}_p << \frac{N_p}{\tau_p}$ then $\frac{N_p}{\tau_p} \approx \phi_p$ and $\frac{N_c}{\tau_c} \approx \phi_c$, where ϕ_p, ϕ_c are spectroscopically measured fluxes. JET data /56/ indicate that

$$\frac{\phi_c}{\phi_p} \approx 0.1$$

$$\rightarrow R_d = 0.96$$

C_d an be obtained from the radial extension of the erosion zone /54/ and the decay lengths of fluxes ($\lambda \sim 0.01$ m). For JET:

$\phi = \phi_0 \, e^{-x/\lambda}$, ϕ_0 flux at last closed flux surface (LCFS), x radial distance from LCFS.

$$\frac{C_e}{C_d} = \frac{\int_0^{0.01} e^{-x/\lambda} dx}{\int_{0.01}^{\infty} e^{-x/\lambda} dx} \qquad (14)$$

With $C_e + C_d = 1$, $C_e = 0.63$, $C_d = 0.37$. From equation (10) $\tau_p^* = \left|\frac{N_p}{\dot{N}_p}\right|$:

$$\tau_p^* = \frac{\tau_p}{C_d(1-R_d)}$$

assuming $\tau_p \approx 0.2$ s for medium density ohmic discharges /56/ $\rightarrow \tau_p^* \approx 14$ s, similar to what has been measured. This is of course a very rough estimate but it shows that H-C-codeposition as a mechanism for H-pumping cannot be ruled out. The fact that only little gas (H) desorbs from the JET walls after a discharge supports this qualitatively. However codeposition alone cannot explain the reversibility of inner wall pumping for instance (codeposition causes permanent losses). To make this work one needs an additional independent gas source at the wall, which fuels the plasma. Measured fluxes of hydrogen from walls might indicate the existence of such a source (plasma induced desorption of hydrogen stored in the walls). However these fluxes can also be simply caused by the recycling of plasma particles. So far no experimental results exist about the importance of C-H-deposition as a pumping mechanism.

iii) Particle Release Due to Auxiliary Heating

As mentioned in section II.3 particle release takes place on a short timescale (< 0.1 s) at the onset of both neutral beam and RF heating. Because of the short timescale it is not believed to be due to an increased power flow into the plasma edge and the subsequent heating of material surfaces /34/. Assuming that the wall and limiter were saturated with hydrogen just before the auxiliary heating, the release mechanism must be such as to provide a new equilibrium between hydrogen released from walls and (edge) plasma flux to the wall during heating. ICRH is known to increase the SOL width as well as the particle energy in the SOL /57/. Neutral Beam injection gives rise to increased charge exchange fluxes in particular from the plasma core. In both cases the energy spectrum of the particles (neutrals and ions) leaving the plasma shifts to higher values and this can cause a particle release by ion induced desorption. Recent investigations on this subject with implantation experiments where particle reemission from saturated carbon was measured after changing the energy of the incident ions suggests an energy dependent saturation concentration on the material surface /58/ which could explain the phenomenon observed in tokamaks.

IV CONCLUSIONS

Recycling phenomena in tokamaks with a large fraction of their walls covered by carbon and with carbon limiters can be separated into two classes. One class comprises phenomena which can be described by known processes between the hydrogen (or helium) and carbon. This is for instance, hydrogen trapping in helium conditioned or previously baked (≥ 350°C) walls, which results either in low density plasmas or requires significantly (≥ 50%) more external gas supply to reach and sustain a certain plasma density compared with discharges with hydrogen conditioned walls. Another example is the plasma induced desorption of wall hydrogen which is caused either by particle (H, He, C) and/or power fluxes (temperature increase) impacting on carbon surfaces. Furthermore, the 100% recycling of helium is also a result which has been known from simulation experiments. All these processes are responsible for the walls to memorise a discharge history. With them, qualitative predictions are possible about the density variations due to wall pumping or wall fuelling processes in a specific discharge provided the previous discharge history is known. For quantitative predictions additional knowledge about the magnitude and the time dependency of particle and power fluxes in the plasma boundary is needed.

The other class comprises recycling phenomena for which the known hydrogen/helium interactions with carbon give no satisfactory explanation. This is particularly true for hydrogen discharges which are reproducible indicating that walls and plasma have come to an equilibrium state, and that the walls and limiters are most likely saturated with hydrogen within the plasma accessible surface layer (some 10-100 nm). However, even under such conditions, an appreciable fraction (≥ 50%) of the input gas is still retained in walls and limiters during the discharge (does not show up in the plasma density). Because there is no saturation effect (equilibrium has been already reached) it must be concluded that there is a continuing exchange of fuel particles between the plasma and material surfaces and that for JET both the plasma and the material surfaces must have a particle retention time of similar order (≤ 0.5 s). Experimentally it is indicated that this particle exchange process is plasma induced (different release time constants with and without plasma, section II.4) and that a fraction of the plasma flux (≤ 10%) does not recycle but is lost. The latter effect (or part of it) can be due to H-C-codepostion but it is also reminiscent of the recycling of hydrogen in tokamaks with metal walls, where part of the incident particles are lost to the bulk material. A global three particle reservoir model gives a satisfactory phenomenological description of various processes under such conditions (fuelling ratio, H-He differences, 'inner wall' pumping) however, without producing an answer about the underlaying physical processes. This makes predictions on recycling in high-power carbon tokamaks (temperature dependency) very difficult and asks for more careful and well-controlled recycling experiments, in particular, in todays large carbon tokamaks. A better understanding will be even more important in the near future when D-T operation requires a stricter particle accountability and density control. Furthermore, the design and the layout of the operational conditions (material, temperature) for the first wall in the next step machines (NET, CIT and ITER) needs also conclusive experimental results on these issues.

ACKNOWLEDGEMENT

The author greatly acknowledges support, contributions and supply of partially unpublished results from members of the JET team as well as from Drs R Behrisch (IPP), S A Cohen (PPPL), H F Dylla (PPPL), G L Jackson (GA), G M McCracken (Culham Laboratories), V Philipps (KFA), W Möller (IPP), W Poschenrieder (IPP), F Waelbroeck (KFA), E Vietzke (KFA).

REFERNCES

/1/ G M McCracken and P E Stott, Nucl Fusion, Vol 19, No 7 (1987) 889.

/2/ H C Howe, J Nucl Mat 93 and 94 (1980) 17.

/3/ S A Cohen, J Ehrenberg, T T C Jones et al, Plasma Physics and Controlled Fusion, Special Issue, Vol 29, No 1017 (1987) 1205.

/4/ F Waelbroeck, D Wienhold and J Winter, J Nucl Mat 111 + 112 (1982) 185.

/5/ K L Wilson and W L Hsu, J Nucl Mat 145-147 (1987) 121.

/6/ D B Heifetz in 'Physics of Plasma-Wall Interactions in Controlled Fusion' ed D E Post and R Behrisch, NATO ASI Series B: Physics Vol 131, Plenum Press, NY, London (1986) 695.

/7/ S A Cohen in 'Physics of Plasma-Wall Interactions in Controlled Fusion' ed D E Post and R Behrisch, NATO ASI Series B: Physics Vol 131, Plenum Press, NY, London (1986) 695.

/8/ H F Dylla and the TFTR Team, J Nucl Mat 145-147 (1987) 48.

/9/ H F Dylla, P H La Marche, M Ulrickson et al, Nucl Fusion, Vol 27, No 8 (1987) 1221.

/10/ G L Jackson, T E Evans, M Ali Mahdavi, Bull Am Phys Soc, 32/9 (1987) 1899.

/11/ M Murakami, J D Callen and L A Berry, Nucl Fusion 16, (1976) 347.

/12/ S J Fieldings, J Hugill, G M McCracken et al, Nucl Fusion 17 (1977) 1382.

/13/ A Gondhalekar, A Cheetham, S A Cohen et al, Bull Am Phy Soc, 32/9 (1987), 1838.

/14/ J Winter, J Nucl Mat 145-147 (1987) 131.

/15/ F Wagner, IPP-Report III/71, August 1981.

/16/ E Vietzke, K Flaskamp, V Philipps et al, J Nucl Mat 145-147 (1987) 443.

/17/ J Winter, J Vac Sci Technol A5(4), July/August (1987) 2286.

/18/ J Winter, H G Esser, F Waelbroeck, P Wienhold, Proc 14th Europ Conf Contr Fusion and Plasma Physics, Madrid, 22-26 June (1987) Vol II, 702.

/19/ K.H. Dippel, K.H Finken, G.J. Thomas, A.E. Pontau, G.A. Campbell, P.M. Goebbel, Proc 12th Europ Conf Contr Fusion and Plasma Physics, Budapest, 2-6 September (1985), Part II, 531.

/20/ T T C Jones et al, this conference.

/21/ M Yoshikowa and the JT-60 Team, Plasma Physics and Controlled Fusion, 28(1986) 165.

/22/ B L Doyle, W R Wampler and D K Brice, J Nucl Mat 103 + 104 (1981) 513.

/23/ R Behrisch, J Ehrenberg, M Wielunski et al, J Nucl Mat 145-147 (1987) 723.

/24/ B Terreault and the TFR Group, J Nucl Mat 127 (1985) 18.

/25/ P H La Marche, H F Dylla, P J McCarthy and M Ulrickson, J Vac Sci Techol A4 (1986) 1198.

/26/ J Ehrenberg, J Nucl Mat 145-147 (1987) 551.

/27/ R A Langley, R S Blever and J Roth, J Nucl Mat 76 + 77 (1978) 313.

/28/ J Ehrenberg, S A Cohen, L de Kock et al, Proc 14th Europ Conf Controlled Fusion and Plasma Phsics, Madrid, 22-26 June 1987, Part II, 706.

/29/ J Winter, H G Esser, F Waelbroeck and P Weinhold, Proc 14 Europ Conf Controlled Fusion and Plasma Physics, Madrid 22-26 June 1987, 702.

/30/ H F Dylla, W R Blanchard, R Budny et al, J Nucl Mat 111 + 112 (1980) 272.

/31/ W L Rowan, C C Klepper, C P Ritz et al, Nucl Fusion 27/7 (1988) 1105.

/32/ S Sengoku and the JFT-2M Team, J Nucl Mat 145-147 (1987) 556.

/33/ D Grosman and the TFR Group, J Nucl Mat 128 + 129 (1984) 292.

/34/ M Bures, V P Bhatnager, M P Evrard et al, Proc 14th Europ Conf Contr Fusion Plasma Physics, Madrid, 22-26 June (1987) Part II, 722.

/35/ J Snipes et al, to be published in Proc 15th Europ Conf Contr Fusion Plasma Physics, Dubrovnik, 16-20 May (1988).

/36/ Y G Wang, W P Poschenrieder and G Venus, J Vac Sci and Technol A4 (1986) 2520.

/37/ W P Poschenrieder, private communication.

/38/ F Dylla et al, this conference.

/39/ H T Nakamura, T Ando, S Niikura et al, JAERI-M 86-173 (1986).

/40/ J Ehrenberg, unpublished results.

/41/ D E Post and C E Singer, J Nucl Mat, 128 + 129 (1984) 78.

/42/ C E Singer in 'Physics of Plasma Wall Interactions in Controlled Fusion ed D E Post and R Behrisch, NATO ASI Series B: Physics Vol 131, Plenum Press, NY, London (1986), 607.

/43/ T Tagle et al, this conference.

/44/ P Morgan, S Corti, J Ehrenberg et al, Proc 12th Europ Conf Contr Fusion Plasma Physics, Budapest 2-6 September 1986, 535.

/45/ G M McCracken and P C Stangeby, Plasma Physics and Controlled Fusion, Vol 27, No 12A (1985), 1411.

/46/ W Möller and J Roth, 'Physics Plasma-Wall Interactions in Controlled Fusion' ed D E Post and R Behrisch, NATO ASI Series B: Physics Vol 131, Plenum Press, NY, London (1986) 439.

/47/ W Engelhardt, F Becker, K Behringer et al, J Nucl Mat, 111 + 112 (1982) 337.

/48/ P C Stangeby, J Nucl Mat 145-147 (1987).

/49/ D E Post, D B Heifetz and M Petravic, J Nucl Mat 111 and 112 (1982) 383.

/50/ P C Stangeby, J A Tagle, S K Erents and C Lowry, Proc 14th Europ Conf Contr Fusion and Plasma Physics, Madrid 22-26 June (1987), Part II, 670.

/51/ P Coad et al, this conference.

/52/ R Langley, J Vac Sci Technol, Vol 5, No 4, Part IV, July/August 1987, 2205.

/53/ R E Clausing, L Heatherley, J Nucl Mat, 145-147 (1987) 317.

/54/ G M McCracken, J Ehrenberg, P E Stott, J Nucl Mat 145-147 (1987) 621.

/55/ W Hsu and R A Causey et al, J Vac Sci and Technol A5(4) (1987) 2768.

/56/ K Behringer, J Nucl Mat 145-147 (1987) 145.

/57/ S A Cohen, D Ruzic, D E Voss et al, Nucl Fusion Vol 24 No 11 (1984) 1490.

/58/ W Möller et al, this conference.

/59/ B M U Scherzer, "Surface topography due to light ion implantation", in 'Sputtering by Bombardment II', ed R Behrisch, Topics in Appl Phys, published by Springer Berlin/Heidleberg/NY (1982).

/60/ R A Causey et al, J Vac Sci Technol A 4(3) (1986) 1189.

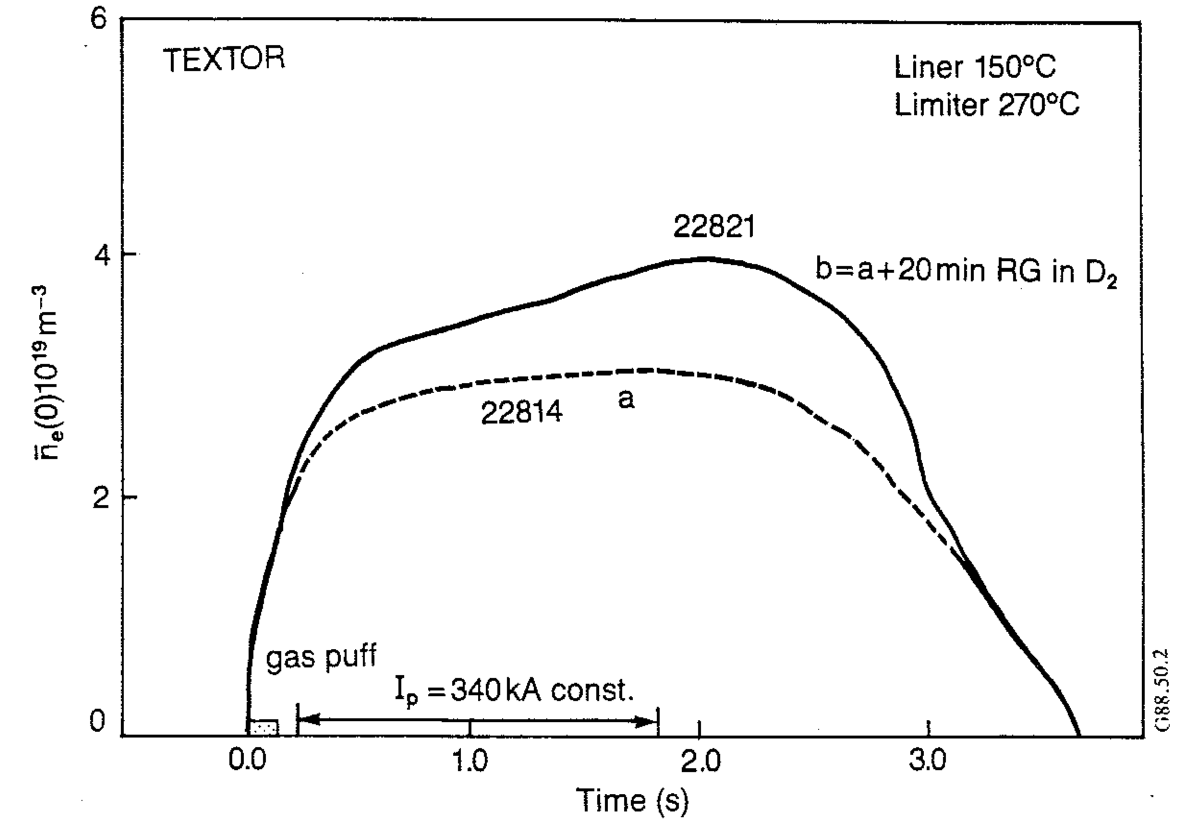

Fig. 1 Plasma density for TEXTOR discharges with $T_w = 150°C$;
(a) discharge 22814 before 20 min of RF-discharge cleaning,
(b)discharge 22821 afterwards.
Hatched box: time of gas puff/17/.

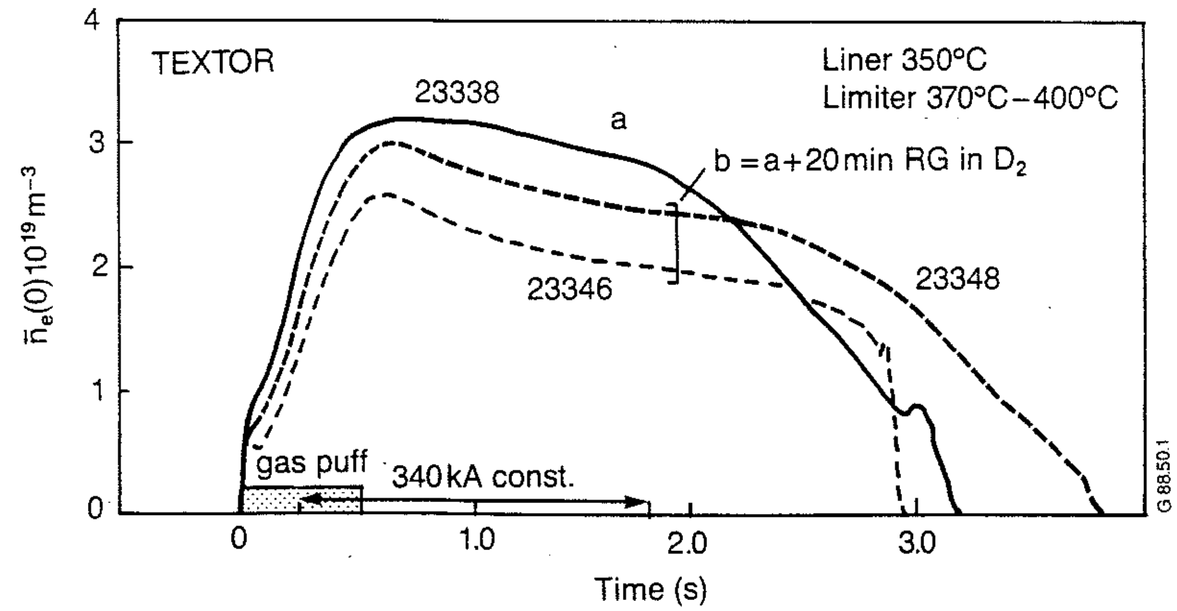

Fig. 2 Plasma density for TEXTOR discharges with $T_W = 350°C$ and $T_L = 370°C - 400°C$, (a) discharge before 20 min of RF discharge cleaning, (b) discharge afterwards /17/.

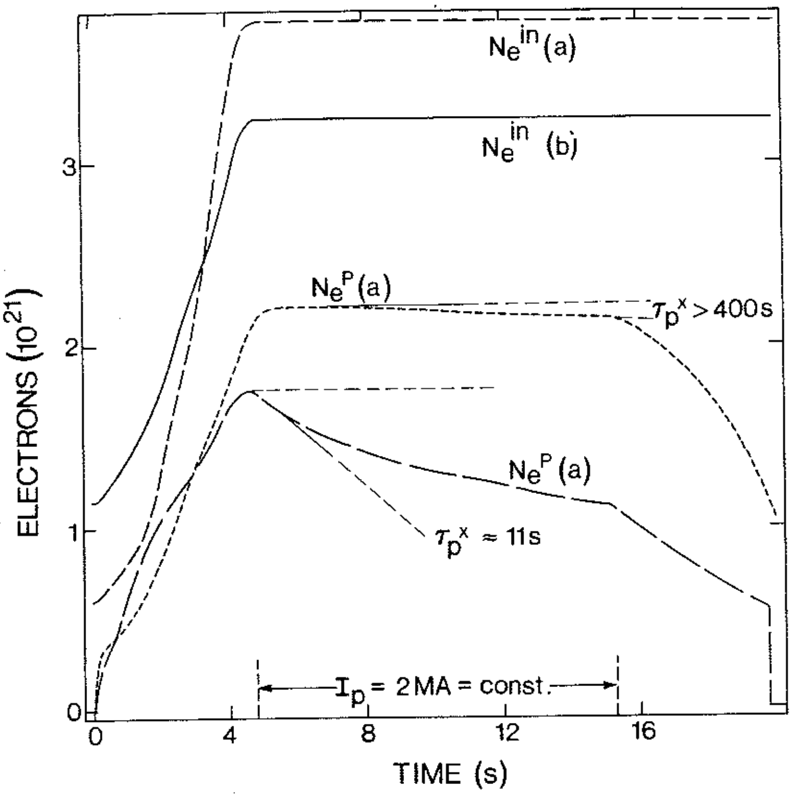

Fig. 3 Gas input and total number of plasma electrons for two JET discharges:
(a) With old (1988) rail limiter configuration and $T_L \approx T_W \approx 300°C$.
(b) With new (1987) belt limiter and $T_L \geq 150°C$, $T_W \approx 300°C$.

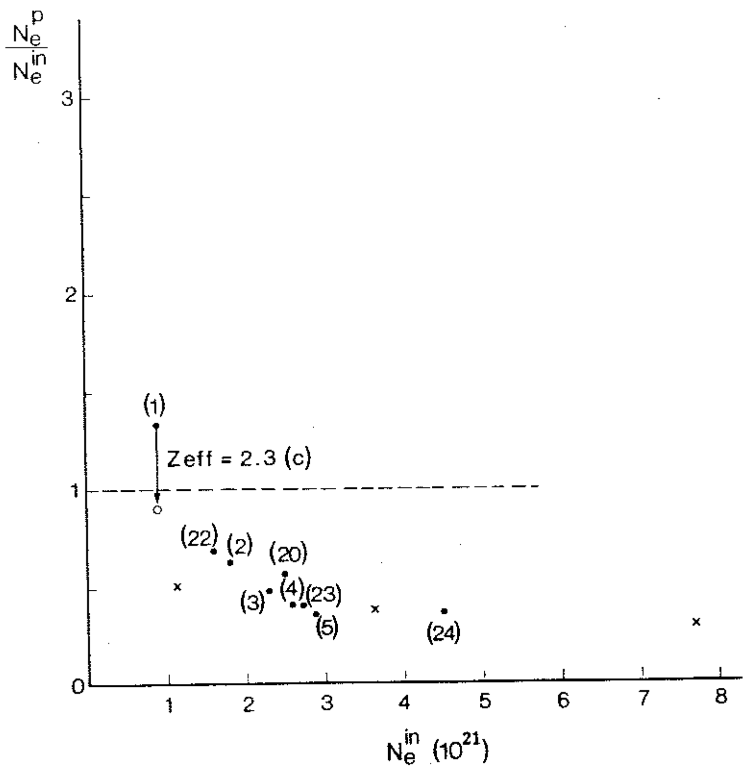

Fig. 4 Fuelling ratio $\frac{N_e^p}{N_e^{in}}$ as a function of N_e^{in} for JET ohmic limiter discharges at $T_L = 100°C$, $T_W = 200°C$. The number denotes the order of the discharge within the discharge series. Correction for Z_{eff} decreases the ratio more at smaller N_e^{in}. N_e^p data were taken at the end of the current flat top (16s in the discharge). $I_p = 2.1$ MA, $B_t = 2.2$ T.

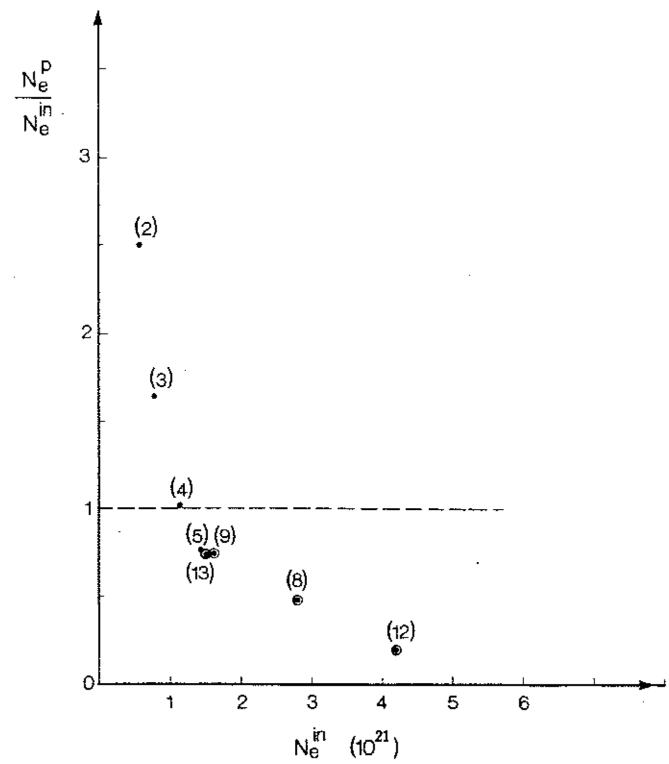

Fig. 5 Fuelling ratio $\frac{N_e}{N_e^{in}}$ as a function of N_e^{in} for JET ohmic discharges with a previous 7.6 h's H-GDC (before #(1)) and with $T_L = T_W = 300°C$.

$I_p = 2MA$, $B_T = 2.2T$

$I_p = 3MA$, $B_T = 2.9T$

Numbers in brackets are sequence numbers.

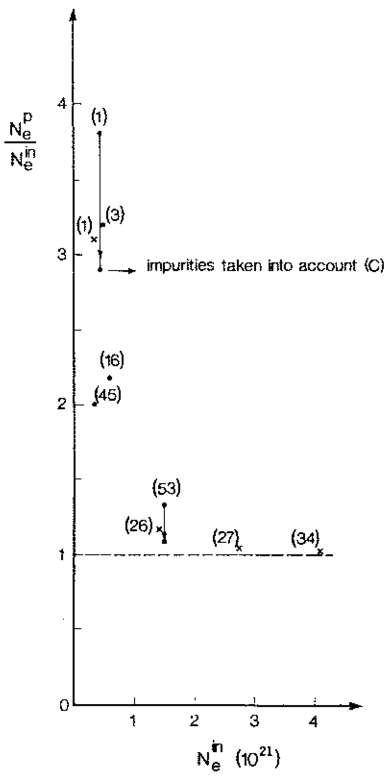

Fig. 6 Fuelling ratio $\frac{N_e^P}{N_e^{in}}$ as a function of N_e^{in} for JET ohmic helium fuelled discharges. Number in brackets are again sequence numbers.

. $T_L = T_W = 200°C$, $I_p = 2.2MA$, $B_T = 3.4T$

x $T_L = T_W = 300°C$, $I_p = 3.2MA$, $B_T = 2.2T$

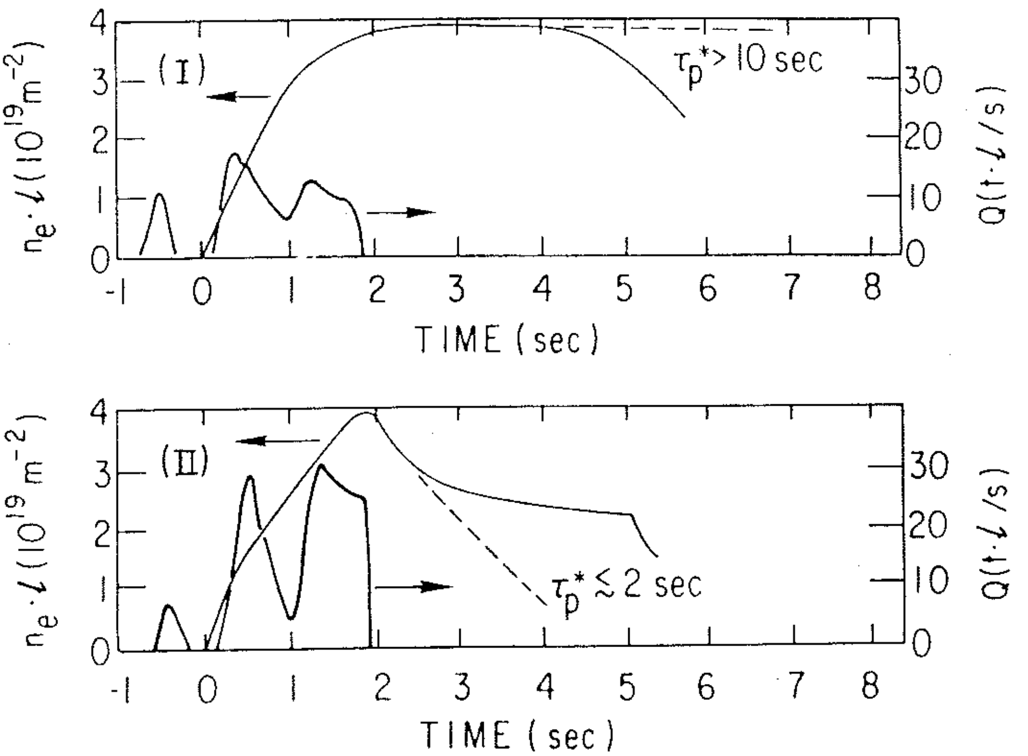

Fig. 7 Comparison of TFTR inner bumper limiter discharges [line integrated central density (ne.L) and external gas supply (Q)] with (II) and without (I) previous Helium conditioning /8/.

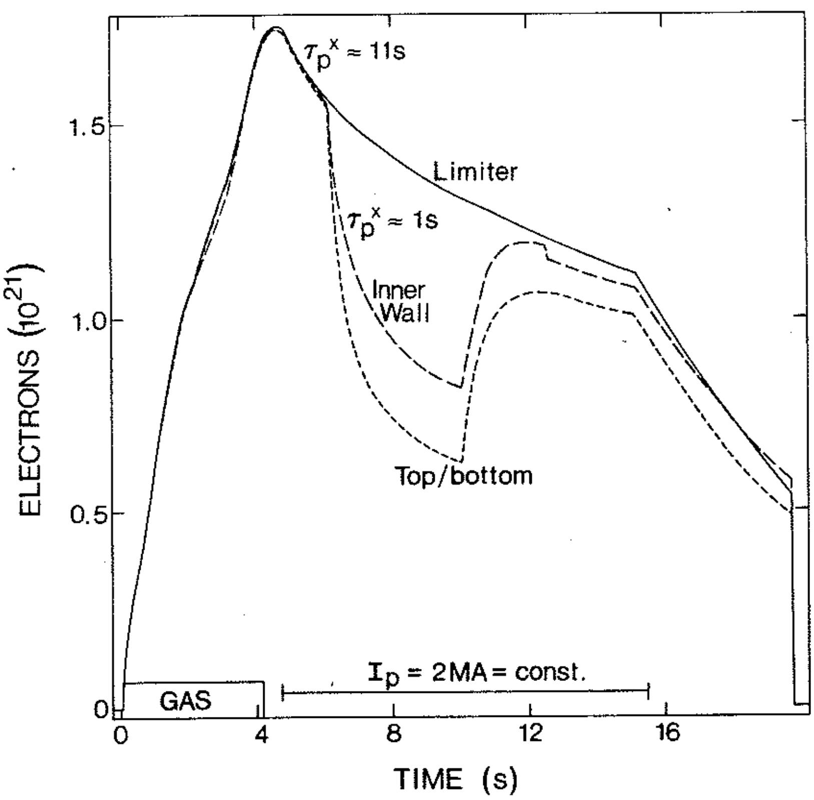

Fig. 8 Variation of the plasma electron content in JET due to plasma position changes. The discharges were identical up to 6 s. The position changes were accomplished within less than 100 ms. At 10 s the plasma was put back onto the limiter. $T_L = 120°C$, $T_W = 200°C$.

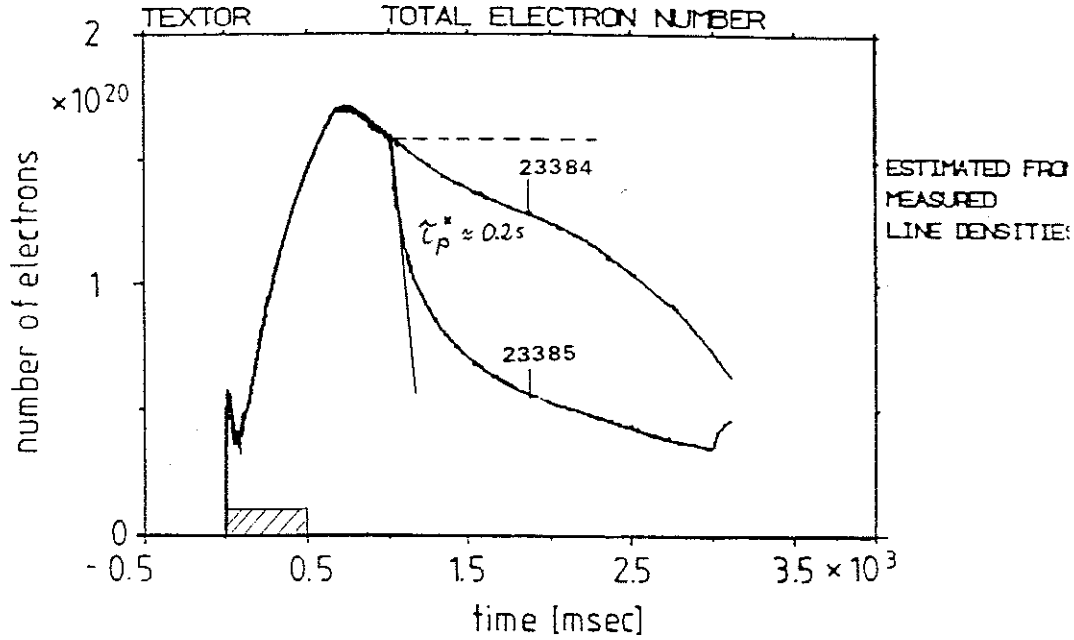

Fig. 9 Plasma pumping in TEXTOR discharges after moving the plasma about 10 cm closer to the inboard wall of the vacuum vessel. Conditions of the vessel were as in Fig. 2, $T_W = 350°C$, $T_L = 370°C - 400°C$ /17/.

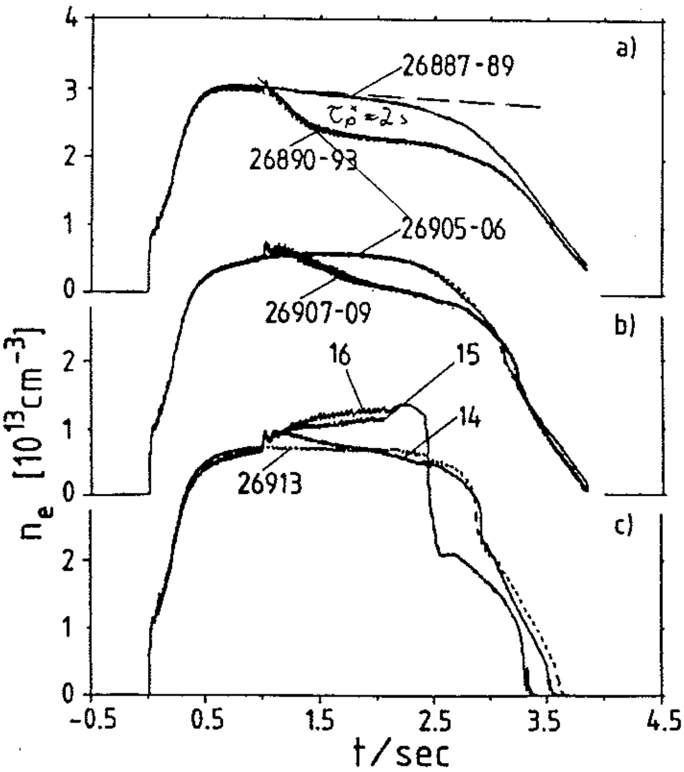

Fig. 10 Same experiment as in Fig. 9 but with $T_W = 150°$ and different previous wall conditioning procedures /29/:

(a) No conditioning (quasi equilibrium)

(b) 5′ RG discharge conditioning in D_2

(c) 10′ RG discharge conditioning in D_2

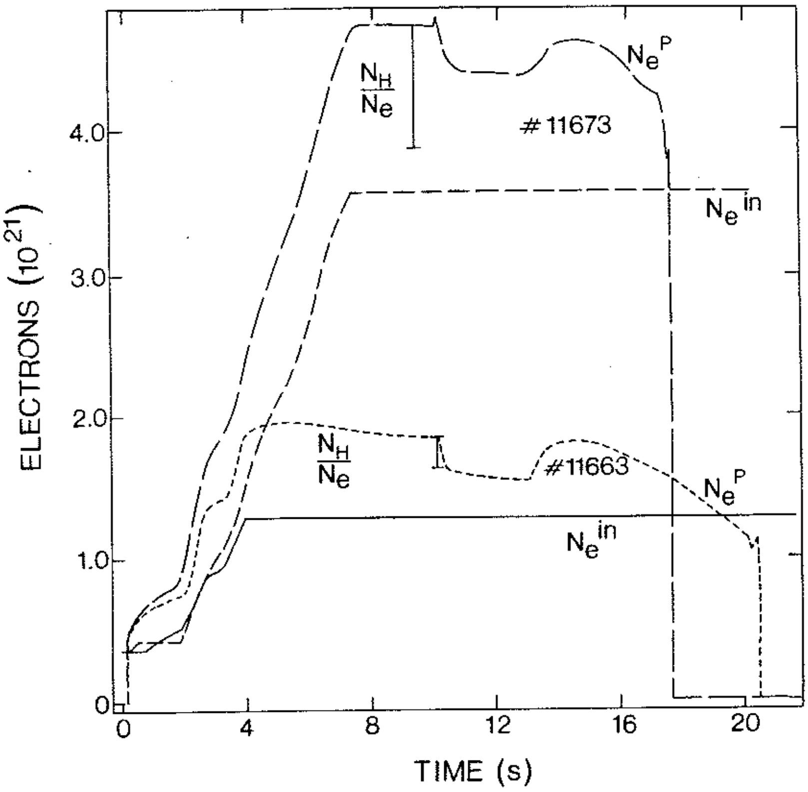

Fig. 11 He fuelled discharges in JET at two different densities. The helium electron input and the total plasma electron content are indicated. At 10 s the plasma was shifted to the inner wall and at 13 s back to the limiter. The residual H content was calculated by assuming 100% fuelling ratio for He and taking into account the measured Z_{eff}, assuming carbon as the only impurity ion. $T_L = T_{W'} = 300°C$.

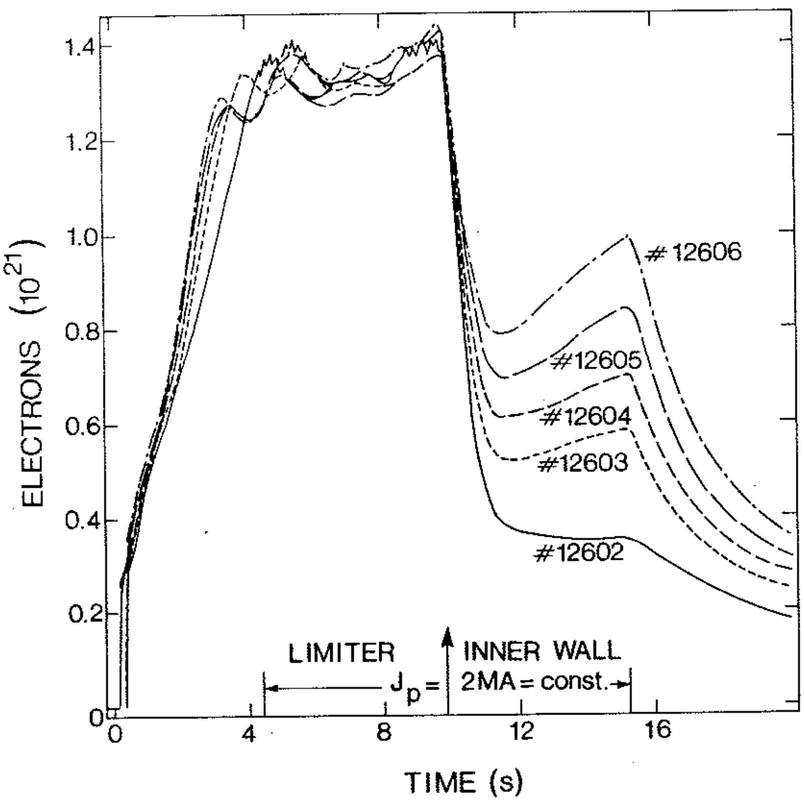

Fig. 12 Electron content evolution (a) of JET deuterium discharges after a series of helium discharges. The discharges were put onto the inner wall at $t = 10$ s, and were then gas fuelled by similar puffs except for #12602.

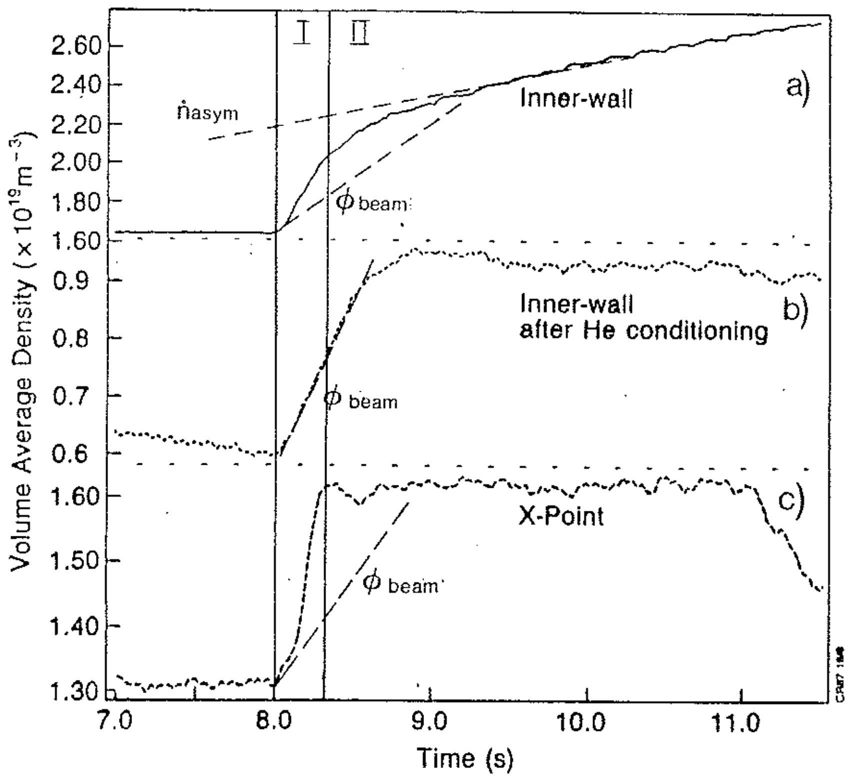

Fig. 13 Density evolution of neutral beam heated discharges in JET for three different conditions as indicated. The transition between phase I and phase II is marked by a decrease or the density rise.

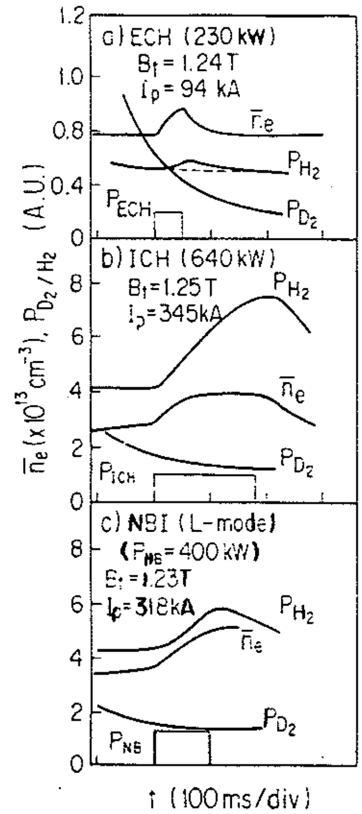

Fig. 14 Partial pressure measurements and density measurements in JFT-2M tokamak during auxiliary heating a)→c). The vessel wall was conditioned with hydrogen and the discharges were performed with deuterium /32/.

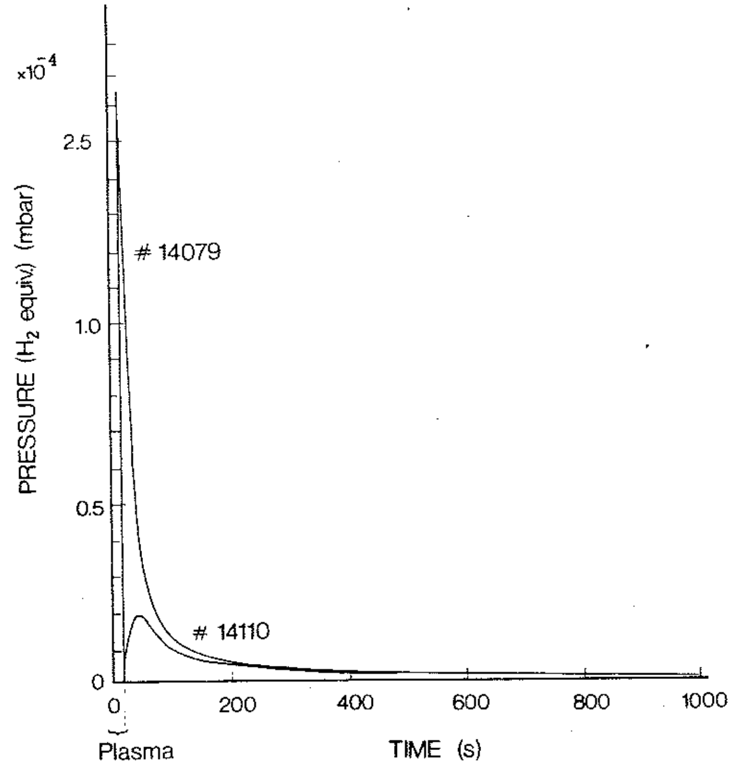

Fig. 15 Comparison of the total pressure evolution (780% D_2) after two different JET discharges:
#14079 disrupted discharge
#14110 soft landed discharge

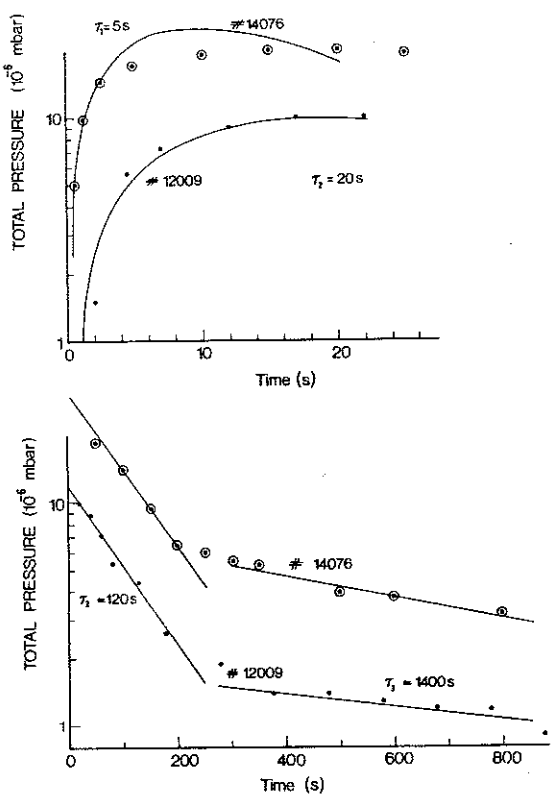

Fig. 16 Evolution of the total pressure after two different discharges in JET. Dots were measured data, curves are calculated data assuming a release process with three different time constants as indicated.

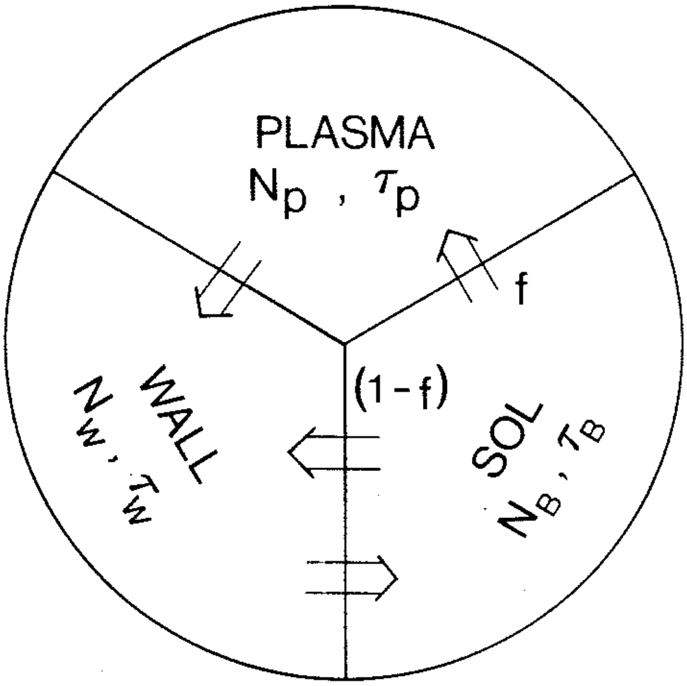

Fig. 17 Schematic of particle fluxes between the three particle reservoirs in a tokamak: the plasma (P), the plasma boundary and SOL (B), and the wall/limiter (W) (details see text).

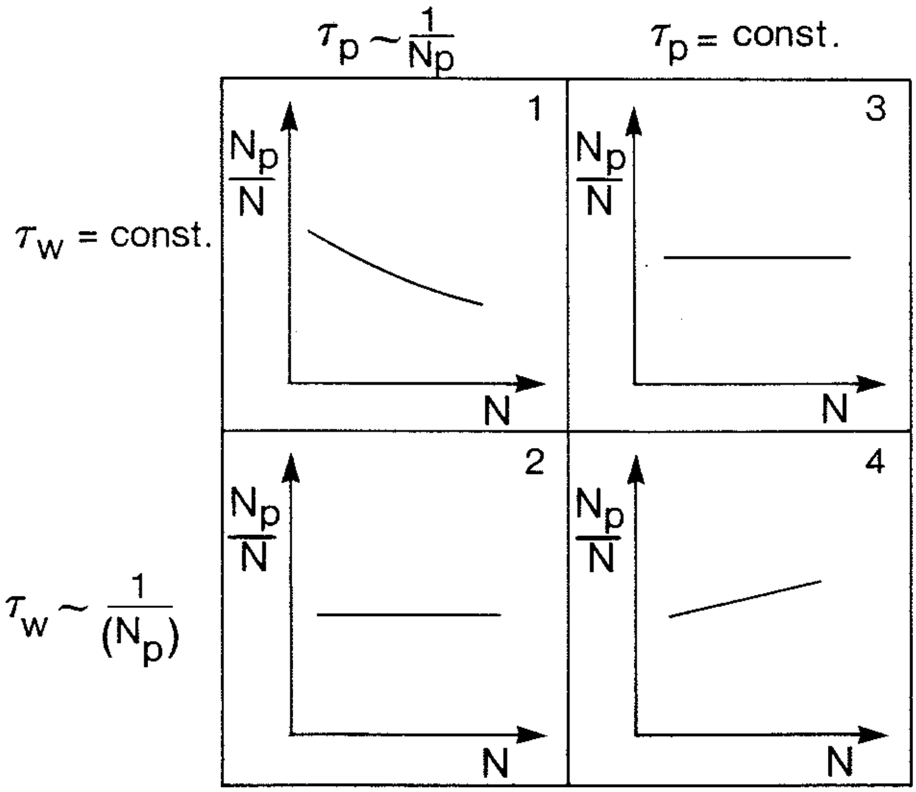

Fig. 18 Calculated qualitative dependency of the fuelling ratio on the total electron input for different combinations of τ_p' and τ_w' (see text).